董丽芳 著

气体放电等离子体动力学

QITIFANGDIAN
DENGLIZITI
DONGLIXUE

河北大学出版社

董丽芳 著

气体放电等离子体动力学

河北大学出版社

气体放电等离子体动力学

图书在版编目(CIP)数据

气体放电等离子体动力学／董丽芳著．－保定：河北大学出版社，2004.10
ISBN 7-81097-066-6
Ⅰ.气… Ⅱ.董… Ⅲ.放电－等离子体动力学－汉、英 Ⅳ.0461
中国版本图书馆CIP数据核字(2004)第009749号

责任编辑：韩 勇
装帧设计：赵 谦
责任印制：闻 利

出版：河北大学出版社
地址：河北保定市合作路88号
经销：全国新华书店
印制：河北新华印刷一厂
规格：1/32 (880mm×1230mm)
印张：11.75
字数：340千字
印数：0001～5000册
版次：2004年10月第1版
印次：2004年10月第1次

前　言

气体放电等离子体动力学，涉及物理学、气体电子学、化学等多个学科，是一个广为引人注目的重要研究领域。其研究成果不仅对气体放电在能源、环境及材料等领域的应用具有重要意义，而且近年来发现气体放电在非线性科学研究中起着重要的作用。本书在对气体放电等离子体动力学研究进行综述的基础上，对作者多年来在此方面的研究成果进行了总结。

本书所涉及到的等离子体包括：介质阻挡放电等离子体、托卡马克等离子体、直流放电等离子体和激光等离子体。

全书共分4章。第1章介绍了介质阻挡放电中的斑图动力学。斑图动力学是非线性科学的一个重要分支，气体放电中的斑图动力学则为目前气体放电动力学的一个前沿领域。作者在独创的水电极介质阻挡放电装置上，率先实现了多种时空斑图，如正方形斑图、准晶斑图、迷宫斑图、点线状斑图等，为斑图动力学提供了一个全新的实验系统。第2章介绍托卡马克等离子体动力学，着重介绍等离子体湍流中相干结构的实验观察及理论分析。第3章介绍直流放电等离子体动力学的数值模拟，特别关注其在金刚石薄膜生长中的应用。第4章介绍激光等离子体化学气相沉积动力学。

本书所包括的研究成果凝聚了尹增谦、贺亚峰、尚勇、刘书华和陈俊英、张玉红、李雪辰、马博琴、张庆利、柴志方、殷燕、王慧娟、王志军、冉俊霞、毛志国、庞学霞、何寿杰、刘富成、李树锋、刘峰、范伟丽等历届博士和硕士研究生的贡献，本书在编写过程中得到了范伟丽、王志军、王慧娟和尹增谦等研究生的很多帮助，作者一并表示衷心的感谢。最后，特别感谢河北大学出版社领导及编辑为本书所付出的辛勤劳动。

由于作者水平有限、时间仓促，错误之处在所难免，恳请读者不吝指正。

著　者

2004.5

目　录

第 1 章　气体放电斑图动力学

斑图(pattern)是在空间或时间上具有某种规律性的非均匀宏观结构,是由系统中微观参量之间的相互作用而导致的宏观量有序分布的状态,是一种典型的非线性自组织现象。它广泛存在于自然科学甚至是社会科学的很多领域,例如自然界中的动物体表花纹、流体中的对流斑图、化学反应中的图灵(Turing)斑图及光学斑图等。另外,从比较均匀对称的胚胎发育成具有多种器官的生物体、神经脉冲的传递、心肌激励以及大脑的活动等也与时空斑图有关。虽然不同系统所显示的斑图结构,不论在时空尺度上,还是在斑图形成的具体机制上,都是各不相同的,但它们在形态上都有一定的相似性。斑图动力学就是研究各种时空结构的自组织形成、选择、演化的动力学共性,目的是搞清微观量是如何相互作用导致宏观量的有序状态,从而达到有效地控制斑图的形成。自 1900 年瑞利(Rayleigh)和贝纳德(Bénard)发现对流斑图,1952 年图灵提出化学反应扩散模型解释动物体表花纹,特别是 1991 年欧阳颀等在实验室实现化学反应扩散图灵斑图以来,斑图动力学在揭示自然界奥妙中的地位及其在各领域的广泛应用前景日益凸现,形成了世界范围的研究热潮,成为各个领域关注的热门学科。

近几年来,介质阻挡放电(简称 DBD)系统作为一个新兴的研究斑图动力学的系统,开始备受国内外研究者的关注[1~8]。介质阻挡放电,又名无声放电,是一个典型的非平衡态交流气体放电过程。其主要特点是电极上覆盖着电介质,电介质的存在会导致电荷积累形成内建电场,因此放电电流与外加电场的关系是非线性的,而放电又远离平衡态,因此介质阻挡放电可以形成斑图。根据不同的放电条件,特别是不同的 pd 乘积值(p 为气体压强,d 为气隙宽度),介质阻挡放电可分为两种不同类型[4]:低 pd 值或外加电压略高于击穿电压时,气体击穿属汤森放电模式;高 pd 值或电压过高时,气体放电为流光模式。在适当

的条件下，两种模式均可出现自组织斑图。与目前研究斑图动力学常用的瑞利—贝纳德系统、化学反应扩散系统等其他系统相比，介质阻挡放电具有如下几方面的优点：(1)放电本身是发光的，因而 DBD 为斑图动力学提供了一个很好的可视化研究对象。(2)DBD 中形成稳定斑图所需要的时间非常短。在一般的非线性耗散系统如流体中热对流系统、化学反应扩散系统中，稳定斑图的形成需要几小时甚至几天的时间，而在 DBD 中只需要几分钟甚至几秒钟[2]。(3)DBD 中构成斑图的单元为放电丝，用我们提出的可选择性光学测量方法可被单独测量，这样可以研究斑图构成单元与斑图的关系。这在其他系统中很难实现。(4)影响斑图模式的控制参数(如外加电压、放电气隙宽度、气体成份等)可以方便地调节。此外，DBD 中的斑图模式有望应用在未来的信息处理[2]、材料的局域生长[3]等方面。因此，对 DBD 中放电斑图动力学进行深入的研究，将推动斑图动力学的发展及放电斑图的应用。

从目前的现状看，由于介质阻挡放电流光模式中斑图难以实现或维持，DBD 斑图动力学的研究大多集中在汤森放电模式，斑图为典型的图灵斑图。在斑图观测方面，美国的 W. Breazel 小组以 He 气加入少量水蒸汽为放电气体，观察到了六边形斑图和条纹斑图[2]。德国的 H. - G. Purwins 研究小组在一系列气体(He、He/Air 等)的介质阻挡放电中，观察到了六边形斑图、条纹斑图、同心圆斑图及六边形与条纹共存的斑图[4~6]。在对斑图的时空动力学测量方面，由于常规的实验方法(照相、电流测量、电荷测量等)不能同时达到高时间分辨率和高空间分辨率，使得这方面的工作进展不大。美国的 M. Walhout 小组用自制的条纹照相机拍照方法，研究了一维介质阻挡放电系统中的斑图的时空动力学[7]。但由于他们实验的时间分辨率为微秒，远远大于放电丝的持续时间(10～100ns)，因而该方法还是不能同时具有高时间分辨率和高空间分辨率。最近德国的 H. - G. Purwins 研究小组采用高速相机研究了同心圆环斑图的时空动力学，但仍为多个周期的时间积分结果，并不是真正意义的时空分辨测量。

本研究小组近几年开展了介质阻挡放电动力学方面的工作，通过采用我们独创的水电极介质阻挡放电装置和清洗放电方法，获得了介

质阻挡放电流光放电模式中的多种时空斑图。除了观察到六边形斑图、条纹斑图及螺旋波斑图以外，还首次在气体放电中实现了正方网格斑图、复合态准晶斑图、点线斑图、迷宫斑图及超六边形斑图等，其中点线斑图在所有斑图研究系统中属首次实现；利用自制的二维可变双通道光学测量装置，首次进行了纳秒(ns)和 0.1mm 尺度上的二维时空相关研究[8~12]。初步测量了正方网格的时空演变，结果发现它是由 2 套网格嵌套而成的，并且还具有时间反演特性。最近，还发现由 2 套、3 套及 4 套网格嵌套而成的运动六边形斑图，这些斑图涉及到了随时间变化的不稳定性问题，揭示了几种新的时空对称性。另外，还发现低气压但高 *pd* 值时，存在如尘埃等离子体中的准粒子、空洞现象。

参考文献

[1]E.L. GureviCh *et al.*, **Phys. Rev. Lett**, 91(15)154501－1～4 (2003).

[2]W. Breazel *et al.*, **Phys. Rev. E**, 52 (2), 1503 (1995).

[3]N. Jiang *et al.*, **Thin solid Films**, 390, 119 (2001).

[4]I. Müller *et al.*, **IEEE Trans. on Plasma Sci.**, 27 (1), 20 (1999).

[5]I. Brauer *et al.*, **Phys. Rev. Lett.**, 84 (18), 4104 (2000).

[6]J. Guikema *et al.*, **Phys. Rev. Lett.**, 85 (18), 3817 (2000).

[7]M. Klein *et al.*, **Phys. Rev. E**, 64,026402 (2001).

[8]L. F. Dong *et al.*, 6th **Asia-Pacific Conf. Plasma Science & Technology**, (invited talk), I－O3, Jeju, Korea, (July, 2002), **Thin solid films** 120,435 (2003).

[9]L. F. Dong et al, **Plasma Sources Science and Technology**, 13 p164 (2004).

[10]L. F. Dong et al, **Plasma Sources Science and Technology**, *12*, 380(2003).

[11]L. F. Dong *et al.*, **Journal of Electrostatics**, 57, 243 (2003).

[12]L. F. Dong *et al*. **Appl. phys. Lett**, 84, 5142 (2004).

1.1 氩气介质阻挡放电斑图动力学

1.1.1 Generation of High-Power-Density Atmospheric Pressure Plasma with Liquid Electrodes

We present a method for generating atmospheric pressure plasma using a dielectric barrier discharge reactor with two liquid electrodes. Four distinct kinds of discharge, including stochastic filaments, regular square pattern, glow-like discharge and Turing stripe pattern, are observed in argon with a flow rate of 9 slm. The electrical and optical characteristics of the device are investigated. Results show that high-power-density atmospheric pressure plasma with high duty ratio in space and time can be obtained. The influence of wall charges on discharge power and duty ratio has been discussed.

Experimental and theoretical studies of atmospheric pressure discharges have been motivated by numerous potential industry applications such as ozone generation, pollution control and sterilization of biological samples[1]. In most applications, plasma with high power density and high duty ratio in space and time is desirable. The most commonly used atmospheric pressure discharge is the dielectric barrier discharge (DBD, also referred to as silent discharge). Recently, H.D.Park *et al* presented the generation of atmospheric pressure plasma with a dual-chamber discharge[2]. L. Mangolini *et al* studied experimentally the spatial structure of dielectric barrier atmospheric pressure glow discharge[3].

In this letter, we present a method for generating high power densi-

ty atmospheric pressure plasma with high duty ratio in space and time. The discharge with a maximum power density of about 14 W/cm^3 and a maximum temporal duty ratio of about 80% has been obtained. In addition, square pattern and stripe pattern have been observed.

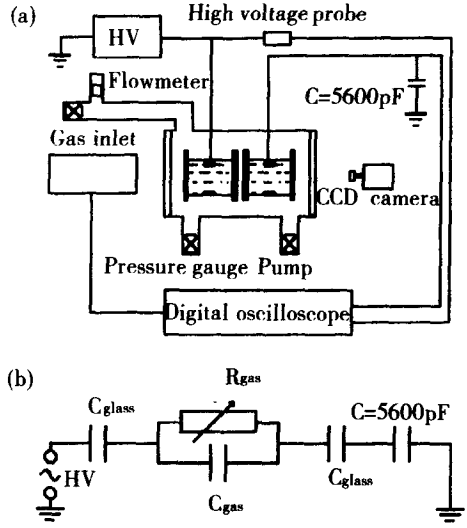

Fig. 1 (a) Schematic diagram of the experimental setup (longitudinal section view of reactor): HV—high voltage high frequency power supply, PMT—photomultiplier tube, (b) The equivalent circuit of the discharge system. For the voltage below breakdown, R_{gas} is estimated to be infinite, C_{gas} is in the order of 10pF and C_{glass} is in the order of 100pF. For the voltage over breakdown, R_{gas} is estimated to be in the order of 100kΩ. The capacitance of equivalent circuit is time-dependent within the cycle of applied voltage.

The experimental device is shown in Fig. 1. Two cylindrical containers with diameters of 46.7mm are filled with tap water without any pretreatment, whose purity is 99.9%. There is a metallic ring immersed

in each of the containers and connected to a power supply. Thus, the water acts as liquid electrode. The parallel glass with thickness of 1.5mm serves as dielectric layer. An ac power supply has a maximum peak voltage of 10kV with frequency of 26kHz. A high voltage probe (Tektronix P6015A, 1000X) is used to measure applied voltage. A capacitor is used to measure the transported charge. The light emitted from the discharge is detected by a PMT (RCA7265) and is recorded with an oscilloscope (Tektronix TDS3054, 500MHz). A digital camera (Canon Powershot G1: 1024×768 pixels, minimum exposure time 1 ms) is used to record images of the discharge. An Ar gas flow of 9 slm is maintained to prevent impurity accumulation during operation.

In the experiments, it is found that the power density and the spatio-temporal duty ratio increase with the increase of applied voltage. Experimentally observed spatial structure, temporal behavior and transported charges of discharge as a function of applied voltage are illustrated in Fig.2. There are four distinct kinds of discharge —— stochastic filaments (Fig.2(a)), regular square pattern (Fig.2(b)), glow-like discharge (Fig.2(c)) and Turing stripe pattern (Fig.2(d)(e)(f)). There are some stochastic filaments when the applied voltage is over the threshold of breakdown. The filament density increases with increasing voltage. A second current spike appears suddenly when the applied voltage reaches a specific value, which is similar to the result presented in Ref.3. Under appropriate conditions, some self-organized patterns such as hexagon pattern and square pattern are formed[4]. The glow-like discharge is formed with continuously increasing voltage. A remarkable characteristic of discharge is current spikes occurring not only at the rising edge but also at the falling edge of applied voltage, what we call discharge before zero voltage. As the applied voltage increases further, Turing stripe pattern appears on the glow-like homogeneous background[5]. Such a Turing pattern has not been reported previously in other DBD systems,

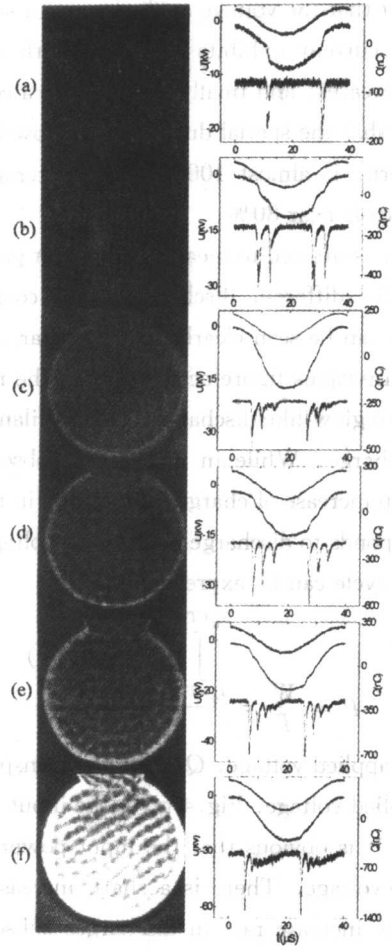

Fig.2 Spatial structure (left column), temporal behavior and transported charges (right column) of discharge vs the applied voltage: (a) stochastic filaments (b) regular square pattern (c) glow-like and (d)-(f) Turing stripe pattern; Waveforms of the applied voltage (top), transported charge (middle) and the total light emission (bottom). The other experimental conditions: frequency $f = 26kHz$, gas gap $d = 1.5$mm, an Ar gas flow of 9 slm, and photographs' exposure time: 1/30s.

likely due to the fact that the voltage applied was not sufficient high. The temporal discharge current exhibits a profile with three spikes, four spikes as voltage increases, and finally evolves into a continuous-like profile. It can be seen that the spatial duty ratio of glow-like discharge, also Turing stripe pattern, is almost 100% and the temporal duty ratio of Turing stripe pattern is near 80%.

Lissajous figure is utilized to measure the input power and results are shown in Fig. 3. for different discharge stages corresponding to that shown in Fig. 2. It can be seen clearly that the sharp increase of charges in lower branch of Lissajous figure occurs only in the range of voltage >0 in discharges prior to glow-like discharge, such as filaments discharge and square pattern discharge. While in discharges subsequent to glow-like discharge, the sharp increase of charges also occurs in the range of voltage < 0, which corresponds to discharge before zero voltage. The power dissipated per voltage cycle can be expressed as

$$P = \frac{W}{T} = \frac{\int_{t_0-T/2}^{t_0+T/2} V(t)dQ(t)}{T}$$

where $V(t)$ is the applied voltage, $Q(t)$ is the transported charge and T is the period of applied voltage. Fig. 4 gives the input power as a function of applied voltage. It is obvious that the input power increases with the increase of applied voltage. There is a sharp increase at glow-like discharge voltage. The increase rate in discharges subsequent to glow-like discharge is larger than that in discharge prior to glow-like discharge. The average power of glow-like discharge turns out to be 10.1W, which corresponds to a power density of $3.9 W/cm^3$. The maximum discharge power is 35.9W, and corresponding power density is $14.0 W/cm^3$. In addition, the Lissajous figure for the voltage below breakdown (not shown here) falls along a line.

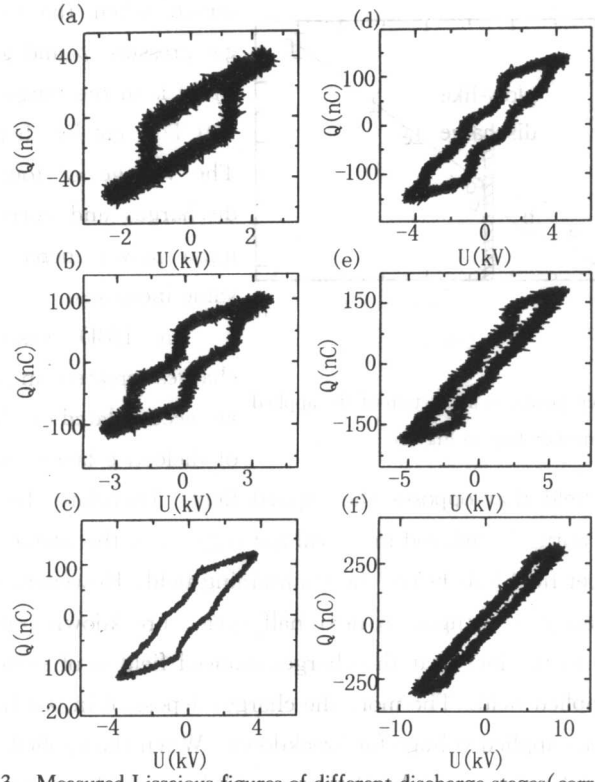

Fig.3 Measured Lissajous figures of different discharge stages(corresponding to Fig.2).

Furthermore, the current is monitored by replacing the test capacitor with a 50 Ω resistor. For the voltage below breakdown, the current is sinusoidal with a $\pi/2$ phase lead and the current is just displacement current. For the voltage over breakdown, the current deviates from the sinusoidal and shows spikes. The current is the superposition of displacement current and gas discharge current. These results are similar to that in other DBD system[2,3].

The four distinct types of discharge (see also Fig.2) could be ob-

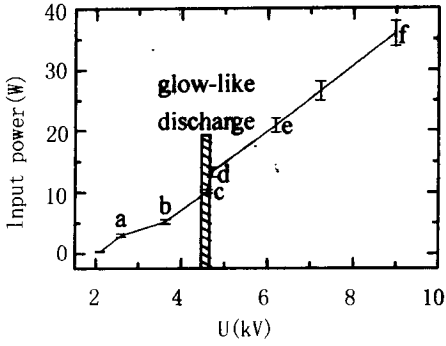

Fig.4 Input power as a function of the applied voltage (corresponding to Fig.2).

served when the product of gas pressure p and gas gap d (pd) is in the range of 100～130 Torr cm by changing d. The voltage of four distinct discharges and corresponding input power increases as pd value increases.

In DBD system, the charges created in discharge are accumulated on the surface of dielectric layer resulting in an electric field that opposes the applied field. Therefore the net field strength is abruptly reduced in a localized region and the filament expires when the net field falls below the maintaining field. However, when the voltage polarity is changed in next half cycle, breakdown occurs more readily due to the fact that the charges-induced field is of same polarity with the applied field. The more the charges deposited in last half cycle, the lower the applied voltage for breakdown. When the applied voltage is sufficient high, the accumulated charges will be more than enough to initiate the reversed gas discharge at the falling edge of the applied voltage. Thus, with a sufficient high voltage, a situation corresponding to discharge subsequent to glow-like discharge in our experiments, the deposited charges will induce discharge at the falling edge of applied voltage. This corresponds to discharge before zero voltage. Obviously, the temporal duty ratio is determined by the extent prior to the instant of zero voltage. The higher the applied voltage, the more time lead prior to the instant of zero voltage and hence the higher the temporal duty ratio. Meanwhile, the deposited charges also influence significantly the input discharge power because they first store the energy at the rising edge of ap-

plied voltage and then release the energy at the falling edge of applied voltage. This can increase the energy conversion efficiency. It would be the origin of a greater ratio between input power and applied voltage in discharge subsequent to glow-like discharge in comparison with that prior to glow-like discharge. In summary, charges deposited on the surface of dielectric layer significantly influence the discharge power and the spatio-temporal duty ratio.

In conclusion, high-power-density atmospheric pressure plasma with high duty ratio in space and time is achieved by using liquid electrodes. The power density and the spatio-temporal duty ratio increase with the increasing voltage. The sharp increase of charges occurs only at rising edge of applied voltage in discharges prior to glow-like discharge. While in discharges subsequent to glow-like discharge, the sharp increase of charges also occurs at falling edge of applied voltage. We propose discharge before zero voltage, which corresponds to the reversed gas discharge initiated by the accumulated charges at the falling edge of applied voltage. Charges deposited on the surface of dielectric layer significantly influence the discharge power and the spatio-temporal duty ratio.

This work is supported by the National Natural Science Foundation of China under Grant No. 10375015, the Key Project of Chinese Ministry of Education. (No. 02020), Committee of Science and Technology, Hebei Province, China under Grant No. 01212180, the Natural Science Foundation of Hebei Province, China under Grant No. A2004000086, and Bureau of Education, Hebei Province, China under Grant No. B2001112.

References

[1] U. Kogelschatz, **IEEE Trans. Plasma Sci.** 30, 1400 (2002).

[2] H. D. Park and S. K. Dhali, **Appl. Phys. Lett.** 77, 2112 (2000).

[3] L. Mangolini, K. Orlov, U. Kortshagen, J. Heberlein and U. Kogelschatz, **Appl.**

Phys. Lett. 80, 1722 (2002).
[4]L.F. **Dong, Z.Q. Yin, L. Wang**, G.S. Fu, Y.F. He, Z.F. Chai and X.C. Li, **Thin Solid Films**, 435, 120 (2003)1.
[5]L.F. Dong, Y.F. He, Z.Q. Yin and Z.F. Chai, **Plasma Sources Sci. Technol.** 13, 164 (2004).

注:原文发表在 **Applied Physics Letters** 84(25) 5142(2004)。

1.1.2 Hexagon and stripe patterns in dielectric barrier streamer discharge

Abstract: We present a specially designed dielectric barrier discharge (DBD) system for the study of pattern formation. Hexagon and stripe patterns have been observed in a streamer discharge in a DBD for the first time. The phase diagram of pattern types as a function of applied voltage is given.

1.1.2.1 Introduction

Pattern formation in systems far from equilibrium is one of the most challenging fields in modern nonequilibrium physics. It has been investigated in systems of different origins, such as chemical, optical and magnetic systems. Recently, much attention has been paid to pattern formation in dielectric barrier discharge (DBD) because it is particularly suited to studies of dynamics of patterns due to simple visualization and convenient experimental timescales[1, 2]. The experimental device of DBD generally consists of two parallel electrodes-at least one of which is covered with a thin dielectric. The discharge type depends on the experimental parameters. For a low product *pd* of gas pressure *p* and gas gap width d, the discharge operates in the Townsend regime leading to a uniform glow discharge. For a high *pd* or overvoltage, the discharge operates in